



Published in final edited form as:

*Biomaterials*. 2015 February ; 41: 26–36. doi:10.1016/j.biomaterials.2014.11.026.

## Linking the foreign body response and protein adsorption to PEG-based hydrogels using proteomics

Mark D. Swartzlander<sup>a,b</sup>, Christopher A. Barnes<sup>c</sup>, Anna K. Blakney<sup>a,†</sup>, Joel L. Kaar<sup>a</sup>, Themis R. Kyriakides<sup>d</sup>, and Stephanie J. Bryant<sup>a,b,e,\*</sup>

Mark D. Swartzlander: Mark.Swartzlander@colorado.edu; Christopher A. Barnes: barnes@biol.bc.ethz.ch; Anna K. Blakney: Blakney@uw.edu; Joel L. Kaar: Joel.Kaar@colorado.edu; Themis R. Kyriakides: Themis.Kyriakides@yale.edu; Stephanie J. Bryant: Stephanie.Bryant@colorado.edu

<sup>a</sup>Department of Chemical and Biological Engineering, University of Colorado, Boulder, CO 80309, USA <sup>b</sup>Biofrontiers Institute, University of Colorado, Boulder, CO 80309, USA <sup>c</sup>Institute of Biochemistry, ETH Zürich, Switzerland <sup>d</sup>Department of Pathology, Yale University School of Medicine, New Haven, CT 06520, USA <sup>e</sup>Material Science and Engineering Program, University of Colorado, Boulder, CO 80309, USA

### Abstract

Poly(ethylene glycol) (PEG) hydrogels with their highly tunable properties are promising implantable materials, but as with all non-biological materials, they elicit a foreign body response (FBR). Recent studies, however, have shown that incorporating the oligopeptide RGD into PEG hydrogels reduces the FBR. To better understand the mechanisms involved and the role of RGD in mediating the FBR, PEG, PEG-RGD and PEG-RDG hydrogels were investigated. After a 28-day subcutaneous implantation in mice, a thinner and less dense fibrous capsule formed around PEG-RGD hydrogels, while PEG and PEG-RDG hydrogels exhibited stronger, but similar FBRs. Protein adsorption to the hydrogels, which is considered the first step in the FBR, was also characterized. *In vitro* experiments confirmed that serum proteins adsorbed to PEG-based hydrogels and were necessary to promote macrophage adhesion to PEG and PEG-RDG, but not PEG-RGD hydrogels. Proteins adsorbed to the hydrogels *in vivo* were identified using liquid chromatography-tandem mass spectrometry. The majority (245) of the total proteins (300) that were identified was present on all hydrogels with many proteins being associated with wounding and acute inflammation. These findings suggest that the FBR to PEG hydrogels may be mediated by the presence of inflammatory-related proteins adsorbed to the surface, but that macrophages appear to sense the underlying chemistry, which for RGD improves the FBR.

\*Corresponding Author: Tel.: +1 303 735-6714, fax: +1 303 492 8425, Address: University of Colorado at Boulder, Department of Chemical and Biological Engineering, UCB 596, Boulder, CO 80303.

<sup>†</sup>Present address: Department of Bioengineering, University of Washington

**Publisher's Disclaimer:** This is a PDF file of an unedited manuscript that has been accepted for publication. As a service to our customers we are providing this early version of the manuscript. The manuscript will undergo copyediting, typesetting, and review of the resulting proof before it is published in its final citable form. Please note that during the production process errors may be discovered which could affect the content, and all legal disclaimers that apply to the journal pertain.

## Keywords

Poly(ethylene glycol); arginine-glycine-aspartic acid (RGD); macrophage; hydrogel; foreign body response; protein adsorption; mass spectrometry

## 1. Introduction

Poly(ethylene glycol) (PEG) hydrogels are being widely investigated for use in implantable devices ranging from coatings on medical devices [1] to scaffolds for cell encapsulation and tissue engineering [2]. They are often considered bioinert because they lack biological recognition. However, their tunable mechanical properties [2] combined with controlled introduction of biological moieties [3] make them highly tailorable to a range of applications. One common biological moiety that has been tethered into PEG hydrogels is the cell adhesion peptide, arginine-glycine-aspartic acid (RGD) [3], which is present in many extracellular matrix (ECM) proteins [4]. RGD modification of PEG hydrogels has recently been used to improve the fundamental understanding of cell-material interactions *in vitro* [5–9]. Furthermore, PEG hydrogels containing immobilized RGD have been investigated for coatings on implantable devices [10] as well as for tissue engineering applications in cartilage, bone, nerve, and the vasculature (e.g., [11–14]). Given their promise, fundamental studies investigating the *in vivo* response to PEG hydrogels with RGD are needed.

Although highly promising, the use of PEG-based hydrogels, as with all non-biological materials [15, 16], is limited by the foreign body response (FBR) that occurs upon implantation [17–20]. *In vitro* we have confirmed that macrophages are capable of adhering to PEG hydrogels in the absence of any cell adhesion ligands, suggesting the presence of adsorbed proteins on the hydrogel surface [17, 21]. We have also reported a strong FBR to PEG hydrogels when implanted subcutaneously into immunocompetent mice as evidenced by a large and persistent presence of macrophages at the hydrogel surface [17, 18]. Interestingly, when RGD ligands are tethered into a PEG hydrogel, the severity of the FBR is reduced, although not abrogated [17, 18]. This observation suggests that biological cues incorporated into a PEG hydrogel may be one strategy to modulate the FBR. However, the mechanisms that mediate the FBR to PEG-based hydrogels need to be elucidated.

Nonspecific protein adsorption to a biomaterial occurs nearly instantaneously upon implantation through a thermodynamically driven process to reduce surface energy [22, 23]. Inflammatory cells are thought to recognize implanted materials as foreign through the adsorbed proteins, thus initiating a cascade of events that lead to the FBR [15]. While hydrophilic materials are often considered resistant to protein adsorption, recent studies have shown that proteins interact with and adsorb to hydrophilic materials. Most notably, studies have shown that fibrinogen interacts with the surface of a PEG-like coating formed by self-assembled monolayers (SAMs) [24]. When a similar PEG-like coating was exposed to a more complex fluid, specifically human blood plasma, a number of proteins were identified that adsorbed to the coating [25]. These findings confirm that proteins are able to adsorb to PEG and therefore may be a critical mediator of the FBR to PEG hydrogels.

Based on the evidence of the FBR to PEG hydrogels in our earlier work and the adsorption of proteins to PEG-based materials, the objectives of this study were two-fold. First, to resolve the mechanisms driving the FBR to PEG hydrogels, the adsorption of proteins to PEG hydrogels was characterized *in vitro* and *in vivo*. In an *in vivo* mouse study, proteins that adsorbed to PEG hydrogels upon subcutaneous implantation were identified using liquid chromatography-tandem mass spectrometry (LC-MS/MS). While several studies have utilized a proteomics-based approach to identify the types of proteins that adsorb to biomaterials *in vitro* (e.g., [25–28]), there is little to no information on the identification of the proteins that adsorb to a biomaterial upon implantation. To the best of our knowledge, this is the first study reporting the identification and characterization of the *in vivo* profile of proteins adsorbed to PEG hydrogels using mass spectrometry proteomics.

The second objective of this study was to elucidate the role by which RGD mediates the FBR to PEG hydrogels. Incorporation of RGD may mediate the FBR to PEG hydrogels via cellular binding of the peptide motif or by altering the profile or presentation of proteins that adsorb to PEG hydrogels. To elucidate the role of RGD in mediating the FBR, three PEG-based materials were investigated: 1) PEG hydrogels, 2) PEG hydrogels immobilized with RGD, and 3) PEG hydrogels immobilized with a scrambled peptide, RDG, which confers similar chemistry as RGD without the bioactivity. Studies were performed on each hydrogel to characterize the FBR, the effects of adsorbed proteins on macrophage adhesion using controlled *in vitro* experiments, and the types of adsorb proteins upon implantation using LC-MS/MS.

## 2. Materials and Methods

### 2.1. Macromer Synthesis

Poly(ethylene glycol) diacrylate (PEG-dA) was synthesized by reacting acryloyl chloride (Sigma-Aldrich, St. Louis, MO), triethylamine (Sigma), and PEG (3000 Da, Fluka, St. Louis, MO) in dry toluene at room temperature protected from light for 16 hours with constant stirring [17]. The product PEG-dA was filtered over alumina, purified by precipitation in cold diethyl ether, dried, and stored at 4°C. The degree of acrylate substitution was confirmed to be 95% by <sup>1</sup>H nuclear magnetic resonance spectroscopy.

The peptides, YRGDS (>95% purity) or YRDGS (>95% purity) (GenScript, Piscataway, NJ) were reacted in 50% molar excess with monoacrylated-PEG-Succinimidyl Carboxymethyl (SCM, 3400 Da from Laysan Bio, Arab, AL or 3500 Da JenKem, Beijing, China) in 50mM sodium bicarbonate buffer (pH 8.4) for two hours. The product acryloyl-PEG-peptide was purified by dialysis then lyophilized. Peptide conjugation was confirmed by <sup>1</sup>H nuclear magnetic resonance spectroscopy to be greater than 95%.

### 2.2. Hydrogel Formation

A macromer solution consisting of 20% (w/w) PEG-dA (3000 Da) and 0.0125% (w/w) photoinitiator, 1-(4-(2-Hydroxyethoxy)-phenyl)-2-hydroxy-2-methyl-1-propane-1-one (I2959, BASF, Tarrytown, NY) with or without 5mM acryloyl-PEG-YRGDS or acryloyl-PEG-YRDGS in phosphate buffered saline (PBS, pH 7.4) was photopolymerized via 365 nm light (10 minutes, 5–10 mW/cm<sup>2</sup>) to produce PEG, PEG-RGD, and PEG-RDG hydrogels.

Under sterile conditions, hydrogel sheets were formed, swollen in PBS, and then punched into disks that were 5 mm in diameter and 0.8 mm in thickness, which were used for both *in vitro* and *in vivo* studies. Over the course of several days, hydrogels were rinsed four times for a minimum of one hour each in sterile filtered 70% ethanol, followed by five rinses for a minimum of one hour each in sterile endotoxin-free PBS. A random sample of hydrogels was selected and confirmed endotoxin-free using the Limulus Amebocyte Lysate test kit (GenScript) prior to implantation. For *in vitro* studies, hydrogel disks were secured to tissue culture treated polystyrene plates using a small amount of sterile vacuum grease. For *in vivo* studies, hydrogel disks were implanted as described below.

### 2.3. Electron Spectroscopy for Chemical Analysis (ESCA)

PEG, PEG-RGD and PEG-RDG hydrogels were dried under high vacuum. A Surface Science Instruments S-probe spectrometer with a monochromatized Al K $\alpha$  X-ray and a low energy electron flood gun for charge neutralization was used for all analyses. The pressure in the analytical chamber was less than  $5 \times 10^{-9}$  Torr. The pass energy was 150 eV. Three X-ray spots ( $\sim 800 \mu\text{m}$ ) were analyzed per sample (PEG, PEG-RGD, and PEG-RDG hydrogels). Spectra were collected at a take-off angle (the angle between the sample normal and the input axis of the energy analyzer) of  $\sim 55^\circ$ , resulting in a sampling depth of 50Å. The Service Physics ESCA2000A Analysis Software was used to determine peak areas and elemental compositions. Si 2p, a contaminating species, was detected on all hydrogels (PEG, PEG-RGD, and PEG-RDG) and determined to be 3.43(0.55)%, 3.30(0.36)%, and 3.80(0.10)%, respectively (mean(SD)). The elemental percentages for C, O, and N were calculated without Si.

### 2.4. In Vivo Implantation

Hydrogel disks were implanted subcutaneously into dorsal pockets of seven-week-old C57BL/6 male mice (Charles River Laboratories) anesthetized with isoflurane (MWI Veterinary Supply Co., Boise, ID) (n=5). Hydrogels were either implanted for 30 minutes for protein adsorption and proteomic studies or 28 days to examine the *in vivo* FBR. An incision was made along the centerline of the back between the shoulder blades and subcutaneous pockets were formed via blunt dissection. For protein adsorption studies, each animal received two implants of the same material. For examining the host response, each animal received four hydrogel discs: one of PEG, PEG-RGD, and PEG-RDG and an additional one of the three materials. The wounds were closed with surgical staples. Mice were monitored daily for abnormalities at the implant site. Animals were sacrificed by CO<sub>2</sub> asphyxiation and cervical dislocation. The implants were excised by removing the dorsal skin and processed either for adsorbed proteins or for histological analysis.

### 2.5. Histological Analysis of the FBR

Dorsal skin with attached explants was pinned in a dissection dish and fixed in 4% paraformaldehyde immediately after explantation. After 24 hours paraformaldehyde was replaced with 15% sucrose and tissue samples were stored at 4°C until dehydration and embedding. Standard protocols were used for dehydration and paraffin embedding.

Histological sections (10  $\mu\text{m}$  thick) were stained with Masson's Trichrome and hematoxylin and eosin (H&E) via standard protocols.

All sections were imaged using light microscopy (Zeiss, Axioskop 40) with a 10x or 20x objective and a digital camera (Diagnostic Instruments, MN 14.2 Color Mosaic) using SPOT Software v. 4.6. Fibrous capsule and inflammatory cell thickness along the dorsal side of the implant were evaluated using NIH ImageJ. Fibrous capsule density, based on collagen staining, was also measured following Zhang *et al.* [29]. In brief, NIH ImageJ was used to determine the intensity of the RGB color across the fibrous capsule in  $\sim 0.5$   $\mu\text{m}$  increments, where an intensity of zero was denoted as white or no staining. The intensity was averaged in 10  $\mu\text{m}$  increments for at least four locations per section and three sections were analyzed per hydrogel. Five biological replicates were analyzed for each hydrogel condition of PEG, PEG-RGD and PEG-RDG hydrogels. The intensity was normalized to the PEG hydrogel at the location closest to the implant (i.e., 0–10  $\mu\text{m}$  location). Data are shown as mean with standard deviation as error bars for  $n=5$  biological replicates.

## 2.6. Protein Adsorption

For *in vitro* protein adsorption, hydrogel disks were soaked in FBS for two hours after which the fluid was removed by aspiration. For *in vivo* protein adsorption, hydrogels were explanted 30 minutes after implantation. In the latter, no excess fluid was visible around the hydrogels. Hydrogels were recovered and placed in 50mM ammonium bicarbonate for two hours and vortexed to remove adsorbed proteins. The samples were subsequently boiled, but no additional proteins were detected. The resulting solutions were snap frozen in liquid nitrogen and stored at  $-80^{\circ}\text{C}$  until further processing. Total protein mass was quantified using the bicinchoninic acid (BCA) assay kit (Pierce) per manufacturer's instructions. Protein (two micrograms/lane) from each hydrogel formulation was run on a 4–20% Tris glycine polyacrylamide gel (BioRad, Hercules, CA). Protein bands were imaged via silver staining (SilverXpress®, Invitrogen) per manufacturer using a VersaDoc MP 4000 Imager (BioRad).

## 2.7. Primary Macrophages

Murine monocytes were isolated from the bone marrow of femora and tibiae of six-week-old C57BL/6 male mice (Charles River Laboratories, Kalamazoo, MI) as described previously [30]. Briefly, cells in bone marrow isolates were separated using Lympholyte M (Accurate Chemical, Westbury, NY). Mononuclear cells were collected and plated on non-tissue culture treated polystyrene in macrophage differentiation medium (IMDM with 20% fetal bovine serum (FBS) (Atlanta Biological, Lawrenceville, GA), 2mM L-glutamine (Invitrogen), penicillin/streptomycin/fungizone (PSF, Invitrogen) and 1.5 ng/ml huM-CSF (R&D Systems, Minneapolis, MN) and 100 ng/ml flt-3 ligand (R&D Systems)) for 10 days. Macrophages were lifted from culture plates using a cell scraper and concentrated via centrifugation.

## 2.8. Macrophage Adhesion

Prior to macrophage seeding, a subset of hydrogels were soaked in FBS for two hours to promote non-specific protein adsorption (serum-containing conditions), while a second

subset of hydrogels were soaked in PBS (serum-free conditions). After which, the fluid was removed by aspiration. Cells were seeded onto the hydrogels at 2,600 cells/mm<sup>2</sup> in 200µL IMDM with PSF and with or without 20% FBS for the serum-containing and serum-free conditions, respectively. This density was chosen, based on previous experience with this cell type, to ensure saturation of macrophage attachment at the hydrogel surface was not reached over the course of 24 hours. Medium was exchanged in both conditions for medium containing 20% FBS after two hours once macrophages appeared attached.

At 24 hours post medium change, cells were fixed in 4% paraformaldehyde for one hour and stored in 15% sucrose at 4°C. Hydrogels were washed twice in PBS and cell membranes permeabilized with 0.1% Triton-X-100 (Sigma) in PBS for five minutes followed by PBS washes. Filamentous actin was stained with fluorescent-labeled phalloidin (Alexa Fluor 546, Invitrogen, 1:30) for 30 minutes followed by nuclear staining with DAPI (Invitrogen, 1:1000). Samples were imaged via laser scanning confocal microscopy with a 10X objective (Zeiss, LSM5 Pascal). A square area (20,000 µm<sup>2</sup>) within each image (4 areas/image) was analyzed in NIH ImageJ software by counting the total number of cells in each square area. A total of three hydrogels were imaged per condition.

## 2.9. Proteomic Analysis

Fifteen micrograms of protein (see section 2.6) were processed from each sample with three biological replicates per hydrogel condition for a total of nine samples for mass spectrometry. Proteins were reduced by adding dithiothreitol (DTT) to a final concentration of 4mM and incubated at 37°C for 30 minutes. The samples were allowed to cool to room temperature, and proteins were alkylated with 14mM iodoacetamide (IDO) and incubated at 37°C for 30 minutes in the dark. IDO was back-quenched with 4mM DTT. Proteins were cleaved via trypsinization overnight at 37°C at a 1:50 (w/w) ratio of trypsin (Promega, Madison, WI) to protein. Samples were desalted with C18 spin columns (Pierce) following the manufacturer's instructions. Proteins were eluted in 40µl of 70% acetonitrile in high purity water for mass spectrometry and speed vacuumed until dry. Tryptic peptides were analyzed using nanoflow ESI-LCMS implementing a Waters nanoAcquity UPLC (Milford, MA) and an LTQ-Orbitrap (Thermo Scientific, Waltham, MA). A 5 hour reversed phase LC gradient was used to separate peptides prior to mass analysis. High resolution MS analysis was performed in the Orbitrap whereas data-dependent MS/MS analysis implementing CID (collision-induced dissociation) was performed in the linear ion trap.

The raw data files were converted to the mzXML format using the converter installed with the Trans-Proteomic Pipeline (TPP) v. 4.7. TPP 4.7 was also used to search peptides using the Comet target/decoy algorithm against the canonical *Mus musculus* reviewed proteome (<http://www.uniprot.org>) containing both forward and reverse sequences used for false discovery rate determination. The parameters file comet.params.high-low (downloaded 6/11/2014) was used for the peptide identification search. Briefly, the parameters include using trypsin as the protease, which was assumed to cleave after lysine (K) and arginine (R). Two missed cleavage sites and one non-tryptic terminus were allowed per peptide. The precursor ion tolerance was set to 20 parts per million (ppm), and fragment ion tolerance was set to 1.0 Dalton. The data were searched with carboxyamidomethylation of cysteine



(+57.0214 amu) residues as a fixed modification and with oxidation of methionine (+15.9949 amu) as a variable modification. Additionally, the final search results were filtered above a 1% false discovery rate using the scoring from the PeptideProphet algorithms part of the TPP 4.7 installation. Results were filtered to include only proteotypic peptides excluding sequences that matched to multiple proteins. For purposes of compiling confident protein lists, protein identifications were only counted if at least one peptide was identified in at least two of the three sample replicates. After filtering, peptide spectra matching to each of the proteins were counted. A normalized spectral count number was computed for each identified protein where spectral counts for each protein were divided by the amino acid sequence length (i.e., number of amino acids) of the same protein as listed in the database [31, 32]. For each sample condition, the top 90% of protein identifications were displayed as a Venn diagram plot.

The Database for Database for Annotation, Visualization and Integrated Discovery (DAVID) v6.7 (<http://david.abcc.ncifcrf.gov/>) [33] was used to assess the biological process and cellular compartment gene ontology terms associated with each of the identified proteins. Proteins were uploaded as gene lists and functional annotation charts were created for the biological process and cellular compartment terms. Percentages of annotated terms per hydrogel sample represent the number of annotated identifications per term divided by the total number of annotated proteins from the input list.

#### 2.10. IACUC

All animal protocols follow the NIH guidelines for the care and use of laboratory animals (NIH Publication #85-23 Rev. 1985), and were approved by the University of Colorado at Boulder Institutional Animal Care and Use Committee.

#### 2.11. Statistical Analysis

Data are presented as mean with standard deviation as error bars of 3–6 replicates as specified. Significance was determined by ANOVA and Tukey's post hoc analysis in KaleidaGraph (Synergy Software, Reading, PA) with  $\alpha=0.05$ . *P*-values less than 0.10 are reported.

### 3. Results

#### 3.1. Hydrogel Characterization

Electron Spectroscopy for Chemical Analysis (ESCA) was used to characterize the surface of PEG, PEG-RGD, and PEG-RDG hydrogels and confirm the incorporation of the tethered peptides. Elemental concentrations are shown in Table 1. A significantly higher amount of nitrogen was detected in the PEG-RGD and PEG-RDG hydrogels when compared to the PEG hydrogels, indicating that RGD and RDG were successfully incorporated. The amount of nitrogen was similar for PEG-RGD and PEG-RDG hydrogels, indicating that approximately equal amounts of RGD and RDG were incorporated into the hydrogels.

### 3.2. Histological Analysis of the In Vivo Host Response

PEG, PEG-RGD, and PEG-RDG hydrogels were implanted subcutaneously for 28 days into immunocompetent mice. Representative histological micrographs of sections stained with hematoxylin and eosin (H&E) to examine the presence of inflammatory cells at the material-tissue interface are shown in Fig. 1a–c. After 28 days, a thick layer of inflammatory cells was present at the material-tissue interface and semi-quantitatively was similar for all three hydrogels (Fig. 1d). Representative histological micrographs of sections stained with Masson's Trichrome to assess fibrous capsule formation by collagen deposition are shown in Fig. 1e–g. Additionally, after 28 days, a fibrous capsule surrounded all hydrogels. The capsule thickness was the lowest around PEG-RGD hydrogels compared to PEG ( $p=0.057$ ) and PEG-RDG ( $p<0.01$ ) hydrogels (Fig. 1h). Collagen density in the capsule was also assessed as a function of distance from the implant revealing a less dense capsule surrounding PEG-RGD hydrogels compared to PEG ( $p<0.0001$ ) and PEG-RDG ( $p<0.0001$ ) hydrogels (Fig. 1i).

### 3.3. In Vitro Protein Adsorption

Adsorption of serum proteins to PEG, PEG-RGD, and PEG-RDG hydrogels was examined for total mass of proteins (Fig. 2a) and protein signature by SDS-PAGE (Fig. 2b). An equivalent amount of adsorbed protein,  $\sim 500 \mu\text{g}/\text{cm}^2$ , was found on all three materials. The signature of the adsorbed proteins as shown by SDS-PAGE was also similar among all three materials with the majority of the protein bands representing proteins larger than 50 kDa.

### 3.4. In Vitro Macrophage Adhesion

Macrophage adhesion to PEG, PEG-RGD, and PEG-RDG hydrogels in the absence and presence of pre-adsorbed proteins (i.e., after soaking in FBS) was assessed by staining for F-actin. Representative confocal microscopy images are shown in Fig. 3a along with counts of the number of adhered cells per surface area for each hydrogel shown in Fig. 3b. In the absence of pre-adsorbed proteins, few macrophages were present at the surface of PEG and PEG-RDG hydrogels, which largely displayed a rounded morphology. In contrast, a large number of surface-adhered macrophages that were spreading were evident on PEG-RGD hydrogels. Macrophage attachment was highest on PEG-RGD hydrogels compared to PEG ( $p<0.001$ ) and PEG-RDG ( $p<0.001$ ) hydrogels whereas cell attachment was greater ( $p=0.09$ ) to PEG-RDG than PEG hydrogels. With pre-adsorbed proteins, macrophage spreading was observed on all three hydrogel surfaces and macrophage adhesion remained highest on PEG-RGD hydrogels ( $p<0.001$  to PEG and  $p<0.01$  to PEG-RDG). Moreover, the presence of pre-adsorbed proteins led to significantly higher macrophage attachment on PEG ( $p<0.001$ ) and PEG-RDG ( $p<0.05$ ) and to a lesser degree on PEG-RGD ( $p=0.08$ ) compared to hydrogels with no pre-adsorbed proteins.

### 3.5. In Vivo Protein Adsorption

The total mass of proteins adsorbed to PEG-RGD and PEG-RDG hydrogels after a 30 minute implantation was similar ( $\sim 75 \mu\text{g}/\text{cm}^2$ ), but was 13–16% lower ( $p<0.05$ ) than PEG (Fig. 4a). The adsorbed proteins were readily removed from the explanted hydrogels via incubation in ammonium bicarbonate buffer with brief agitation. Notably, incubating the



hydrogels at elevated temperature (i.e., via boiling) did not alter the amount of protein that was extracted. The signature of the adsorbed proteins as shown by SDS-PAGE was also similar among all three hydrogels (Figure 4b), like the *in vitro* adsorption experiments. As seen in the *in vitro* adsorption experiments, the majority of the protein bands represent proteins larger than 50 kDa.

### 3.6. Proteomic Analysis on In Vivo Adsorbed Proteins

The adsorbed protein profile for each of the explanted hydrogels was identified using LC-MS/MS proteomics. To assess the total number of identified proteins per hydrogel, proteotypic peptides were compiled excluding identified peptides whose sequences matched to multiple protein IDs. Additionally, only proteins with at least one proteotypic peptide identified in at least two of the three replicate hydrogels per formulation were counted. By doing so, peptides that originated from 370, 349, and 391 proteins for the PEG, PEG-RGD, and PEG-RDG hydrogels, respectively, were identified. A full list of protein identifications, which encompasses proteins identified in all runs for each hydrogel condition, is provided in Supplemental Table 1. In Figure 5a, the top 90% of the total number of identified proteins for each hydrogel formulation is displayed as a Venn diagram to illustrate the similarities among the different hydrogels. Out of more than 300 proteins that were identified for each hydrogel formulation, 245 proteins were present on all hydrogels. These 245 common proteins represent 66%, 70%, and 63% of the total identifications for the PEG, PEG-RGD, and PEG-RDG hydrogels, respectively.

To assess the levels of each of the identified proteins, a normalized spectral counting method was used for each run where the number of MS spectra matching to a particular protein was divided by the total amino acid sequence length of that protein. Proteins that were identified more frequently resulted in a higher normalized spectral count value suggesting a higher overall abundance of the proteins. At least sixteen of the twenty highest scoring proteins adsorbed to PEG hydrogels were also found adsorbed to PEG-RGD and PEG-RDG (Fig. 5b). Of these sixteen, serum albumin was consistently observed at levels far above the rest of the proteins and was similar among all hydrogel formulations. Fig. 5b depicts the normalized spectral counts data for the cumulative protein list that represent the top 20 identifications for each hydrogel, totalling 24 proteins. A similarity in spectral counts across the various conditions is seen for all top identifications.

Within the top 20 identified proteins in Figure 5b, several proteins were assigned the cellular compartment (CC) gene ontology (GO) term “extracellular space” (GO:0005615) and included for example albumin, apolipoprotein A-I, vitamin D-binding protein, hemopexin, and alpha-2-macroglobulin. In all, 41%, 42%, and 39% of the total identified proteins from the PEG, PEG-RGD, and PEG-RDG hydrogels, respectively, were annotated with the extracellular space term (Table 2) using the GO annotations with the DAVID gene ontology (<http://david.abcc.ncifcrf.gov>) online tool [33]. Additionally, protein identifications for each condition were matched to the biological process (BP) GO terms (Table 3). The top six most represented GO BP terms were identical for each condition. These annotations were: response to wounding, proteolysis, defense response, immune response, inflammatory response, and acute inflammatory response. Additionally, positive regulation of response to

stimulus was seen in the top 10 of each condition. Interestingly, nearly 30 proteins for each condition were identified which have been associated with the *in vivo* response to organic substance.

#### 4. Discussion

In this study, we demonstrated that proteins readily adsorb to PEG-based hydrogels and that the adsorbed proteins mediate macrophage adhesion to the hydrogels. The presence of RGD or RDG in the hydrogel did not influence the amount of protein adsorption *in vitro*, although led to slightly, yet significantly, lower levels *in vivo*, but did not influence the profile of the adsorbed proteins in *in vitro* and *in vivo* adsorption studies. However, we confirmed the FBR to PEG hydrogels is influenced by the presence of RGD, leading to an overall less dense and thinner fibrous capsule, which is consistent with our previous reports [17, 18]. This effect appeared to be due to cellular recognition of RGD as a scrambled sequence, RDG, resulted in a FBR that was similar to PEG hydrogels with no peptide. While the FBR to PEG-based hydrogels is likely mediated through surface-adsorbed proteins, the inclusion of a peptide ligand is able to alter the long-term outcome of the FBR and, in the case of RGD, improve the FBR by reducing the fibrous capsule.

Although protein adsorption is generally low on hydrophilic materials due to their low surface energy in aqueous environments, proteins, as has been reported [24, 25, 34], may still adsorb to hydrophilic materials. We confirmed in this study that proteins readily adsorb to PEG hydrogels that are formed from PEG-dA macromers *in vitro* and *in vivo*. PEG hydrogels formed from these macromers are highly water-swollen polymeric networks that consist of hydrophobic polyacrylate chains connected by hydrophilic PEG crosslinks [35]. Protein interactions with PEG hydrogels may occur through hydrophobic interactions with polyacrylate chains, although, for the hydrogel formulation used in this study, polyacrylate chains comprise only ~1% of the total hydrogel mass. Alternatively, protein interactions with the hydrogel may occur through hydrogen bonding between PEG and protein molecules [36]. Several studies have shown that blood plasma proteins are capable of adsorbing to PEG brushes [25, 34], which was attributed to the formation of hydrogen bonds between PEG and amide groups in the polypeptide backbone of the proteins [36]. While it has been shown that water molecules form an ordered layer around crosslinked PEG, the ordering of water at the solution-solid interface only partially reduces protein adsorption [37].

Because of the highly water swollen nature of hydrogels, proteins may diffuse into the hydrogel in addition to being adsorbed on the surface. Interestingly, the amount of proteins adsorbed to the hydrogels in this study *in vitro* and *in vivo* is greater than what is estimated for a protein monolayer [38]. However, estimation of the mesh size of the hydrogel used, which is ~45Å [19], suggests that the majority of the proteins identified via mass spectrometry analysis are too large to diffuse into the hydrogel. Additionally, it was previously shown that, in the case of similar hydrogels, albumin (~67 kDa), which is the most abundant protein in human serum, is restricted to the hydrogel surface [39]. Given that the protein signature from adsorption studies indicated that the majority of the adsorbed proteins are albumin and larger than albumin, the proteins identified are most likely present

at the hydrogel surface. Accordingly, we hypothesize that multiple protein layers may form on the hydrogel surface, which may be facilitated by the nature of the interaction of protein molecules with PEG and surface-associated water. Specifically, the interaction of proteins with PEG hydrogels in their native state may facilitate a larger extent of protein packing at the interface [22]. Additionally, protein molecules may be entrapped within the layers of structured water molecules in the near-hydrogel surface environment [40]. We observed that most proteins were easily removed by a saline wash, suggesting the proteins are loosely adsorbed and multiple protein layers may therefore exist at the hydrogel surface.

In *in vitro* experiments, pre-adsorption of serum proteins to PEG hydrogels had a significant effect on macrophage adhesion. Indeed, few macrophages adhered to PEG hydrogels in the absence of pre-adsorbed proteins, confirming that non-specifically adsorbed proteins mediate macrophage adhesion to PEG hydrogels. Macrophage adhesion was significantly higher on PEG-RGD hydrogels with pre-adsorbed proteins when compared to PEG-RDG and PEG hydrogels. Since protein mass and signature were similar among all hydrogels, these *in vitro* findings suggest that macrophages can sense the underlying RGD chemistry despite the presence of proteins covering the hydrogel surface. Notably, in the absence of pre-adsorbed proteins, an increase in macrophage adhesion was observed with the incorporation of RGD, confirming macrophage recognition of RGD, which is in agreement with previous reports [41].

To determine if the presence of RGD or RDG affects the protein adsorption profile *in vivo*, proteins that adsorbed to implanted PEG hydrogels were identified via proteomic analysis. While RGD and RDG alter the surface chemistry slightly and introduce an overall net negative charge to the hydrogel, all three explanted hydrogel conditions had remarkably similar protein adsorption profiles based on mass spectrometry profiling. The most identified protein in all three conditions was albumin, a well-known major component of plasma that floods the interstitial space upon implantation. Overall, there was a high prevalence of extracellular space proteins and proteins involved in various wound response mechanisms. Indeed, many of the top proteins identified have been previously reported in murine wound exudates [42, 43] and known to be involved in the acute phase of inflammation [44].

As the process of implanting the PEG hydrogels causes a wound, the presence of many acute inflammatory phase proteins is not surprising. However, others have previously reported that many proteins associated with acute inflammation are detected in chronic wounds [43]. Therefore, the composition of the proteins in combination with their persistent presence at the PEG hydrogel surface may initiate and sustain a FBR. Several of the top proteins identified are known regulators of wound healing. These proteins include apolipoprotein A-I, which inhibits cytokine release in macrophages, and alpha-2-macroglobulin ( $\alpha_2M$ ) and murinoglobulin-1, which are broad protease inhibitors [45]. Interestingly, in addition to inhibiting proteases, the protein  $\alpha_2M$  binds and regulates the activity and transport of cytokines and growth factors, including the pro-inflammatory cytokine interleukin-1 [45]. Hemopexin, which was also identified, regulates inflammation and inhibits IL-6 and TNF- $\alpha$  secretion in LPS stimulated macrophages [46]. Ceruloplasmin is a plasma protein that is elevated during inflammation and has been shown to possess

antioxidant activity [47]. Although proteins associated with fibrin clot formation, including plasminogen, were also detected, such proteins were accompanied by anti-thrombin III, a regulator of clot formation.

On the contrary, several of the top proteins identified have known roles in stimulating inflammation. For example, vitamin D binding protein, which is the precursor to macrophage activating factor that leads to macrophage activation [48], enhances phagocytosis in macrophages similar to the protein alpha-2-HS-glycoprotein [48, 49]. Serotransferrin is an iron binding transport protein, which can also be oxidized by reactive oxygen species and has been shown to further stimulate inflammation [50]. Extracellular plasma hemoglobin can lead to reactions associated with oxidative stress and, without regulators like hemopexin, tissue damage [51]. Although normally present in serum, at elevated levels, the fatty-acid binding protein adipocyte has been linked to inflammation and fibrosis [52]. Complement component 3 (C3) was detected on all three hydrogels, which can be activated by implanted biomaterials to initiate the alternative complement pathway [53, 54]. C3 has been reported to bind to several biomaterials *in vitro* and *in vivo* [55–58], promoting monocyte adhesion [59] and contributing to the FBR to implanted biomaterials [60]. Other studies have shown that *in vitro* PEG-like materials are capable of activating C3 [61]. Other complement proteins were present, including complement component 8, which is involved in the formation of the membrane attack complex.

Several other proteins were identified for which their role, if any, in mediating the FBR is less clear. For example, carbonic anhydrase III, which is present in many tissues, is involved in transport and metabolic processes within cells, but can be released upon tissue injury [62, 63]. Creatine kinase M-type, which is an enzyme that is present in tissues with high energy demands, like muscle, can be oxidized by reactive oxygen species and released from cells [64]. Several predominantly intracellular proteins were present and included fructose-bisphosphate aldolase A, which is involved in actin polymerization [65], and four and a half LIM domains protein 1 (FHL1), which is important in the maintenance of and signaling in skeletal muscle [66]. The exact role of zinc-alpha-2-glycoprotein is not known, but it has been linked to the immune response [67]. Overall there were more than 300 proteins identified, which were adsorbed to each of the hydrogels and which may have contributed to the FBR.

The most abundant proteins adsorbed to PEG-based hydrogels span from those involved in inflammation to regulators of inflammation and wound healing. When compared to *in vitro* studies of adsorbed proteins from human blood plasma onto PEG-OH SAM surfaces [25], many of the proteins that were identified *in vitro* were also identified in this study; although, many more proteins were identified in our *in vivo* study. Given that the FBR occurs in response to all three hydrogels investigated in this study and macrophages persist through the four week implantation, it is likely that the balance between inflammatory proteins and regulatory proteins favors inflammation. While the exact nature of which proteins mediate the FBR to PEG hydrogels remains to be determined, the proteomic analysis presented here provides new insight into the specific proteins that are present at the surface of PEG hydrogels.

Our results confirm that incorporation of the cell adhesion peptide RGD reduces the fibrous capsule density and thickness associated with the FBR to PEG hydrogels. Although proteins readily adsorb to PEG-based hydrogels, the identity of the proteins was nearly identical regardless of the presence of RGD or RDG. Our findings, moreover, suggest that the inflammatory cells, most notably macrophages, responsible for orchestrating the FBR are able to sense the underlying RGD chemistry. This observation may result from direct binding to RGD or possibly through the retention of the native structure of proteins that adsorb to PEG-RGD hydrogels, unlike to PEG or PEG-RDG hydrogels, on which adsorbed proteins may unfold. Consistent with the former, RGD was shown to reduce the inflammatory cascade at the early stages of lung injury and this response was attributed to RGD binding to  $\alpha_v$  integrin on inflammatory cells [68] and therefore the FBR may in part be mediated by the type of integrins that are engaged when inflammatory cells interrogate PEG hydrogels. While RGD is able to attenuate the FBR, the FBR is not abrogated and therefore additional studies are needed to identify ways that better control and prevent the FBR. This study nonetheless supports the idea that peptide ligands recognized by cells can be incorporated into a PEG hydrogel and can elicit a biological response despite protein adsorption to the hydrogel surface.

## 5. Conclusions

We have examined protein adsorption and the FBR to PEG-based hydrogels *in vitro* and *in vivo*. This study to the best of our knowledge presents the first identification of the types of proteins that adsorb to PEG hydrogels, specifically formed from 20% (w/w) PEG-dA macromers, upon subcutaneous implantation. Using mass spectrometry, the adsorbed proteins to PEG-based hydrogels included many known to be involved in the acute phase of inflammation. Several of the proteins identified are known activators of macrophages, such as alpha-2-HS-glycoprotein, vitamin D binding protein and complement component 3. While proteins cover the hydrogel surface, we demonstrate that macrophages can sense the underlying chemistry and in particular with the incorporation of a cell adhesion peptide, RGD, the fibrous capsule density and thickness is significantly reduced. This finding is attributed in part to the bioactivity of RGD, since the scrambled peptide (RDG) having the same chemistry, but lacking bioactivity, did not show the same effect, even though it exhibited similar protein adsorption.

## Supplementary Material

Refer to Web version on PubMed Central for supplementary material.

## Acknowledgments

Research reported in this publication was supported by the the National Institute of Dental and Craniofacial Research under Award Number 1R03DE019505 and by the National Institute of Arthritis and Musculoskeletal and Skin Diseases of the National Institutes of Health under Award Number 1R21AR064436. The surface analysis experiments performed at NESAC/BIO were supported by NIH grant number EB-002027 from the National Institute of Biomedical Imaging and Bioengineering. Mass spectrometry was performed by Jeremy Balsbaugh at the Central Analytical Laboratory at the University of Colorado at Boulder.

## References

1. Bridges AW, Garcia AJ. Anti-inflammatory polymeric coatings for implantable biomaterials and devices. *J Diabetes Sci Technol*. 2008; 2:984–94. [PubMed: 19885288]
2. Nicodemus GD, Bryant SJ. Cell Encapsulation in Biodegradable Hydrogels for Tissue Engineering Applications. *Tissue Engineering Part B*. 2008; 14:149–65.
3. Hern DL, Hubbell JA. Incorporation of adhesion peptides into nonadhesive hydrogels useful for tissue resurfacing. *J Biomed Mater Res*. 1998; 39:266–76. [PubMed: 9457557]
4. Hersel U, Dahmen C, Kessler H. RGD modified polymers: biomaterials for stimulated cell adhesion and beyond. *Biomaterials*. 2003; 24:4385–415. [PubMed: 12922151]
5. Huebsch N, Arany PR, Mao AS, Shvartsman D, Ali OA, Bencherif SA, et al. Harnessing traction-mediated manipulation of the cell/matrix interface to control stem-cell fate. *Nat Mater*. 2010; 9:518–26. [PubMed: 20418863]
6. Yao X, Peng R, Ding JD. Cell-Material Interactions Revealed Via Material Techniques of Surface Patterning. *Adv Mater (Weinheim, Ger)*. 2013; 25:5257–86.
7. Wang X, Yan C, Ye K, He Y, Li Z, Ding J. Effect of RGD nanospacing on differentiation of stem cells. *Biomaterials*. 2013; 34:2865–74. [PubMed: 23357372]
8. Salierno MJ, Garcia AJ, del Campo A. Photo-Activatable Surfaces for Cell Migration Assays. *Adv Funct Mater*. 2013; 23:5974–80.
9. Cao B, Peng R, Li Z, Ding J. Effects of spreading areas and aspect ratios of single cells on dedifferentiation of chondrocytes. *Biomaterials*. 2014; 35:6871–81. [PubMed: 24840616]
10. Petrie TA, Raynor JE, Dumbauld DW, Lee TT, Jagtap S, Templeman KL, et al. Multivalent integrin-specific ligands enhance tissue healing and biomaterial integration. *Sci Transl Med*. 2010; 2:45ra60.
11. Villanueva I, Weigel CA, Bryant SJ. Cell-matrix interactions and dynamic mechanical loading influence chondrocyte gene expression and bioactivity in PEG-RGD hydrogels. *Acta Biomater*. 2009; 5:2832–46. [PubMed: 19508905]
12. Yang F, Williams CG, Wang DA, Lee H, Manson PN, Elisseff J. The effect of incorporating RGD adhesive peptide in polyethylene glycol diacrylate hydrogel on osteogenesis of bone marrow stromal cells. *Biomaterials*. 2005; 26:5991–8. [PubMed: 15878198]
13. McKinnon DD, Kloxin AM, Anseth KS. Synthetic hydrogel platform for three-dimensional culture of embryonic stem cell-derived motor neurons. *Biomaterials Science*. 2013
14. Jimenez-Vergara AC, Guiza-Arguello V, Becerra-Bayona S, Munoz-Pinto DJ, McMahon RE, Morales A, et al. Approach for fabricating tissue engineered vascular grafts with stable endothelialization. *Ann Biomed Eng*. 2010; 38:2885–95. [PubMed: 20464634]
15. Anderson JM, Rodriguez A, Chang DT. Foreign body reaction to biomaterials. *Semin Immunol*. 2008; 20:86–100. [PubMed: 18162407]
16. Ratner BD, Bryant SJ. Biomaterials: Where we have been and where we are going. *Annu Rev Biomed Eng*. 2004; 6:41–75. [PubMed: 15255762]
17. Lynn AD, Kyriakides TR, Bryant SJ. Characterization of the in vitro macrophage response and in vivo host response to poly(ethylene glycol)-based hydrogels. *Journal of Biomedical Materials Research Part A*. 2010; 93A:941–53. [PubMed: 19708075]
18. Lynn AD, Blakney AK, Kyriakides TR, Bryant SJ. Temporal progression fo the host response to implanted poly(ethylene glycol) based hydrogels. *Journal of Biomedical Materials Research Part A*. 2011; 96A:621–31. [PubMed: 21268236]
19. Blakney AK, Swartzlander MD, Bryant SJ. The effects of substrate stiffness on the in vitro activation of macrophages and in vivo host response to poly(ethylene glycol)-based hydrogels. *Journal of Biomedical Materials Research Part A*. 2012; 100A:1375–86. [PubMed: 22407522]
20. Swartzlander MD, Lynn AD, Blakney AK, Kyriakides TR, Bryant SJ. Understanding the host response to cell-laden poly(ethylene glycol)-based hydrogels. *Biomaterials*. 2013; 34:952–64. [PubMed: 23149012]



21. Lynn AD, Bryant SJ. Phenotypic changes in bone marrow-derived murine macrophages cultured on PEG-based hydrogels activated or not by lipopolysaccharide. *Acta Biomater.* 2011; 7:123–32. [PubMed: 20674808]
22. Zhou HX, Rivas GN, Minton AP. Macromolecular crowding and confinement: Biochemical, biophysical, and potential physiological consequences. *Annual Review of Biophysics.* 2008; 37:375–97.
23. Franz S, Rammelt S, Scharnweber D, Simon JC. Immune responses to implants - A review of the implications for the design of immunomodulatory biomaterials. *Biomaterials.* 2011; 32:6692–709. [PubMed: 21715002]
24. Kastantin M, Langdon BB, Chang EL, Schwartz DK. Single-molecule resolution of interfacial fibrinogen behavior: effects of oligomer populations and surface chemistry. *J Am Chem Soc.* 2011; 133:4975–83. [PubMed: 21391676]
25. Riedel T, Riedelova-Reicheltova Z, Majek P, Rodriguez-Emmenegger C, Houska M, Dyr JE, et al. Complete identification of proteins responsible for human blood plasma fouling on poly(ethylene glycol)-based surfaces. *Langmuir.* 2013; 29:3388–97. [PubMed: 23391268]
26. Kim JK, Scott EA, Elbert DL. Proteomic analysis of protein adsorption: serum amyloid P adsorbs to materials and promotes leukocyte adhesion. *J Biomed Mater Res A.* 2005; 75:199–209. [PubMed: 16082704]
27. Backovic A, Huang HL, Del Frari B, Piza H, Huber LA, Wick G. Identification and dynamics of proteins adhering to the surface of medical silicones in vivo and in vitro. *J Proteome Res.* 2007; 6:376–81. [PubMed: 17203981]
28. Sund J, Alenius H, Vippola M, Savolainen K, Puustinen A. Proteomic characterization of engineered nanomaterial-protein interactions in relation to surface reactivity. *ACS Nano.* 2011; 5:4300–9. [PubMed: 21528863]
29. Zhang L, Cao ZQ, Bai T, Carr L, Ella-Menye JR, Irvin C, et al. Zwitterionic hydrogels implanted in mice resist the foreign-body reaction. *Nat Biotechnol.* 2013; 31:553. [PubMed: 23666011]
30. Jay SM, Skokos E, Laiwalla F, Krady MM, Kyriakides TR. Foreign body giant cell formation is preceded by lamellipodia formation and can be attenuated by inhibition of Rac1 activation. *Am J Pathol.* 2007; 171:632–40. [PubMed: 17556592]
31. Hauri S, Wepf A, van Drogen A, Varjosalo M, Tapon N, Aebersold R, et al. Interaction proteome of human Hippo signaling: modular control of the co-activator YAP1. *Mol Syst Biol.* 2013; 9:713. [PubMed: 24366813]
32. Paoletti AC, Parmely TJ, Tomomori-Sato C, Sato S, Zhu DX, Conaway RC, et al. Quantitative proteomic analysis of distinct mammalian Mediator complexes using normalized spectral abundance factors. *Proc Natl Acad Sci U S A.* 2006; 103:18928–33. [PubMed: 17138671]
33. Huang DW, Sherman BT, Lempicki RA. Systematic and integrative analysis of large gene lists using DAVID bioinformatics resources. *Nat Protoc.* 2009; 4:44–57. [PubMed: 19131956]
34. Gunkel G, Huck WT. Cooperative adsorption of lipoprotein phospholipids, triglycerides, and cholesteryl esters are a key factor in nonspecific adsorption from blood plasma to antifouling polymer surfaces. *J Am Chem Soc.* 2013; 135:7047–52. [PubMed: 23581703]
35. Wu J, Lin W, Wang Z, Chen S, Chang Y. Investigation of the hydration of nonfouling material poly(sulfobetaine methacrylate) by low-field nuclear magnetic resonance. *Langmuir.* 2012; 28:7436–41. [PubMed: 22512533]
36. Hasek J. Poly(ethylene glycol) interactions with proteins. *Z Kristallogr.* 2006:613–8.
37. Leung BO, Yang Z, Wu SSH, Chou KC. Role of Interfacial Water on Protein Adsorption at Cross-Linked Polyethylene Oxide Interfaces. *Langmuir.* 2012; 28:5724–8. [PubMed: 22390193]
38. Horbett, TA. The role of adsorbed proteins in tissue response to biomaterials. In: Ratner, BD.; Hoffman, AS.; Schoen, FJ.; Lemons, JE., editors. *Biomaterials Science: An Introduction to Biomaterials in Medicine.* San Diego, CA: Elsevier Academic Press; 2004. p. 237-46.
39. Weber LM, Lopez CG, Anseth KS. Effects of PEG hydrogel crosslinking density on protein diffusion and encapsulated islet survival and function. *Journal of biomedical materials research Part A.* 2009; 90:720–9. [PubMed: 18570315]
40. Vogler EA. Structure and reactivity of water at biomaterial surfaces. *Adv Colloid Interface Sci.* 1998; 74:69–117. [PubMed: 9561719]

41. Schmidt, DR.; Waldeck, H.; Kao, WJ. Protein Adsorption to Biomaterials. In: Puleo, DA.; Bizios, R., editors. *Biological Interactions on Material Surfaces*. New York: Springer; 2009. p. 2-17.
42. Escalante T, Rucavado A, Pinto AF, Terra RM, Gutierrez JM, Fox JW. Wound exudate as a proteomic window to reveal different mechanisms of tissue damage by snake venom toxins. *J Proteome Res*. 2009; 8:5120–31. [PubMed: 19764775]
43. Fernandez ML, Broadbent JA, Shooter GK, Malda J, Upton Z. Development of an enhanced proteomic method to detect prognostic and diagnostic markers of healing in chronic wound fluid. *Br J Dermatol*. 2008; 158:281–90. [PubMed: 18070206]
44. Gabay C, Kushner I. Mechanisms of disease: Acute-phase proteins and other systemic responses to inflammation. *N Engl J Med*. 1999; 340:448–54. [PubMed: 9971870]
45. Rehman AA, Ahsan H, Khan FH. alpha-2-Macroglobulin: a physiological guardian. *J Cell Physiol*. 2013; 228:1665–75. [PubMed: 23086799]
46. Liang XY, Lin T, Sun GJ, Beasley-Topliffe L, Cavaillon JM, Warren HS. Hemopexin down-regulates LPS-induced proinflammatory cytokines from macrophages. *J Leukoc Biol*. 2009; 86:229–35. [PubMed: 19395472]
47. Chapman AL, Mocatta TJ, Shiva S, Seidel A, Chen B, Khalilova I, et al. Ceruloplasmin is an endogenous inhibitor of myeloperoxidase. *J Biol Chem*. 2013; 288:6465–77. [PubMed: 23306200]
48. Homma S, Yamamoto M, Yamamoto N. Vitamin-D-binding protein (group-specific component) is the sole serum-protein required for macrophage activation after treatment of peritoneal-cells with lysophosphatidylcholine. *Immunol Cell Biol*. 1993; 71:249–57. [PubMed: 8225394]
49. Jersmann HP, Dransfield I, Hart SP. Fetuin/alpha2-HS glycoprotein enhances phagocytosis of apoptotic cells and macropinocytosis by human macrophages. *Clin Sci (Lond)*. 2003; 105:273–8. [PubMed: 12725640]
50. Thanan R, Oikawa S, Yongvanit P, Hiraku Y, Ma N, Pinlaor S, et al. Inflammation-induced protein carbonylation contributes to poor prognosis for cholangiocarcinoma. *Free Radic Biol Med*. 2012; 52:1465–72. [PubMed: 22377619]
51. Schaer DJ, Buehler PW, Alayash AI, Belcher JD, Vercellotti GM. Hemolysis and free hemoglobin revisited: exploring hemoglobin and hemin scavengers as a novel class of therapeutic proteins. *Blood*. 2013; 121:1276–84. [PubMed: 23264591]
52. Milner KL, van der Poorten D, Xu A, Bugianesi E, Kench JG, Lam KS, et al. Adipocyte fatty acid binding protein levels relate to inflammation and fibrosis in nonalcoholic fatty liver disease. *Hepatology*. 2009; 49:1926–34. [PubMed: 19475694]
53. Andersson J, Ekdahl KN, Larsson R, Nilsson UR, Nilsson B. C3 adsorbed to a polymer surface can form an initiating alternative pathway convertase. *J Immunol*. 2002; 168:5786–91. [PubMed: 12023380]
54. Nilsson B, Ekdahl KN, Mollnes TE, Lambris JD. The role of complement in biomaterial-induced inflammation. *Mol Immunol*. 2007; 44:82–94. [PubMed: 16905192]
55. Andersson J, Ekdahl KN, Lambris JD, Nilsson B. Binding of C3 fragments on top of adsorbed plasma proteins during complement activation on a model biomaterial surface. *Biomaterials*. 2005; 26:1477–85. [PubMed: 15522749]
56. Sperling C, Maitz MF, Talkenberger S, Gouzy MF, Groth T, Werner C. In vitro blood reactivity to hydroxylated and non-hydroxylated polymer surfaces. *Biomaterials*. 2007; 28:3617–25. [PubMed: 17524475]
57. Chenoweth DE. Complement activation in extracorporeal circuits. *Ann N Y Acad Sci*. 1987; 516:306–13. [PubMed: 3439733]
58. Hed J, Johansson M, Lindroth M. Complement activation according to the alternate pathway by glass and plastic surfaces and its role in neutrophil adhesion. *Immunol Lett*. 1984; 8:295–9. [PubMed: 6526424]
59. Wang X, Schmidt DR, Joyce EJ, Kao WJ. Application of MS-Based Proteomics to Study Serum Protein Adsorption/Absorption and Complement C3 activation on Poly(ethylene glycol) Hydrogels. *J Biomater Sci Polym Ed*. 2011; 22:1343–62. [PubMed: 20594411]
60. McNally AK, Anderson JM. Complement C3 participation in monocyte adhesion to different surfaces. *Proc Natl Acad Sci U S A*. 1994; 91:10119–23. [PubMed: 7937848]

61. Szott LM, Stein MJ, Ratner BD, Horbett TA. Complement activation on poly(ethylene oxide)-like radiofrequency glow discharge-deposited surfaces. *J Biomed Mater Res A*. 2011; 96:150–61. [PubMed: 21105163]
62. Henry RP. Multiple roles of carbonic anhydrase in cellular transport and metabolism. *Annu Rev Physiol*. 1996; 58:523–38. [PubMed: 8815807]
63. Harju AK, Booterabi F, Kuuslahti M, Supuran CT, Parkkila S. Carbonic anhydrase III: A neglected isozyme is stepping into the limelight. *J Enzyme Inhib Med Chem*. 2013; 28:231–9. [PubMed: 22803676]
64. Brioschi M, Polvani G, Fratto P, Parolari A, Agostoni P, Tremoli E, et al. Redox Proteomics Identification of Oxidatively Modified Myocardial Proteins in Human Heart Failure: Implications for Protein Function. *PLoS ONE*. 2012; 7
65. Kusakabe T, Motoki K, Hori K. Mode of interactions of human aldolase isozymes with cytoskeletons. *Arch Biochem Biophys*. 1997; 344:184–93. [PubMed: 9244396]
66. Shathasivam T, Kislinger T, Gramolini AO. Genes, proteins and complexes: the multifaceted nature of FHL family proteins in diverse tissues. *J Cell Mol Med*. 2010; 14:2702–20. [PubMed: 20874719]
67. Hassan MI, Waheed A, Yadav S, Singh TP, Ahmad F. Zinc alpha 2-glycoprotein: a multidisciplinary protein. *Mol Cancer Res*. 2008; 6:892–906. [PubMed: 18567794]
68. Moon C, Han JR, Park HJ, Hah JS, Kang JL. Synthetic RGDS peptide attenuates lipopolysaccharide-induced pulmonary inflammation by inhibiting integrin signaled MAP kinase pathways. *Respir Res*. 2009; 10:18. [PubMed: 19272161]

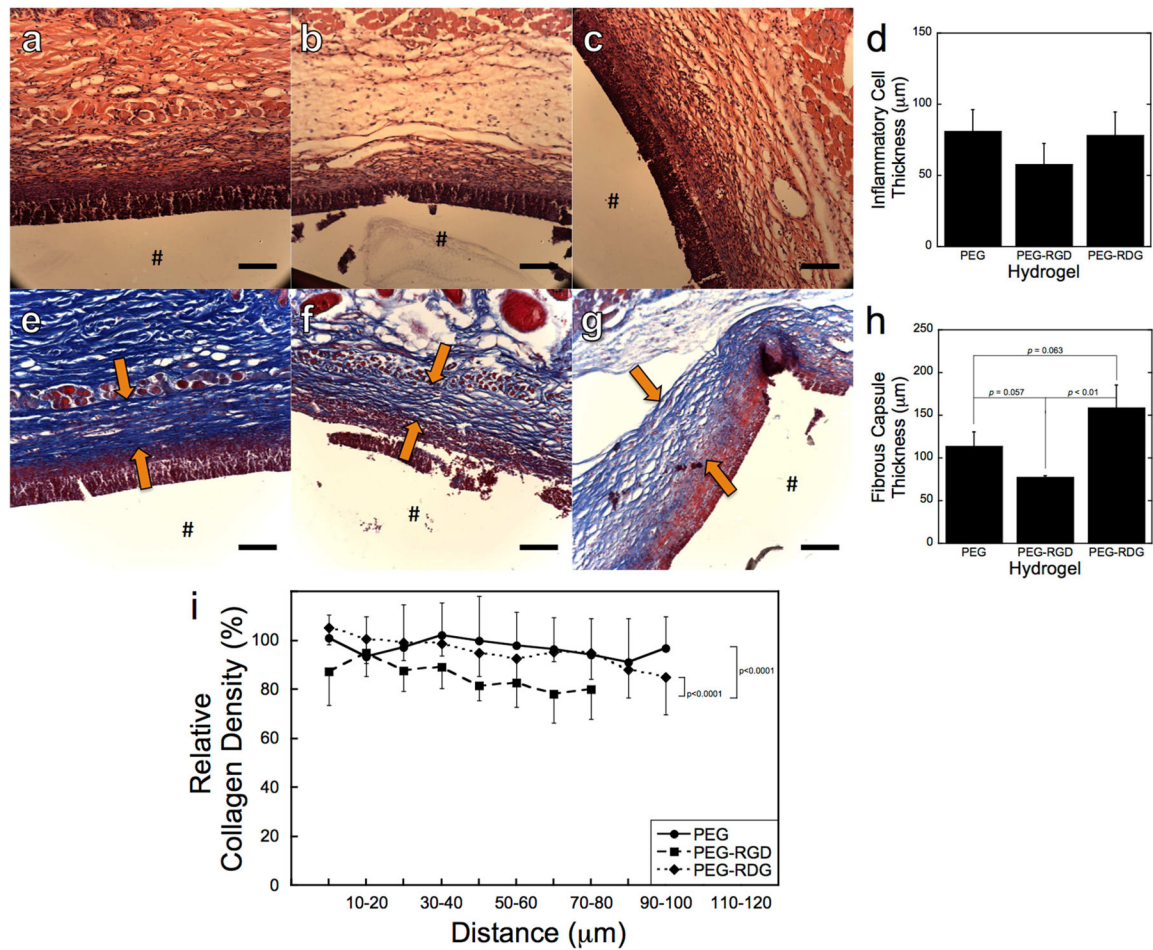


**Figure 1.** Representative histological images of the *in vivo* response to PEG (a, e), PEG-RGD (b, f), and PEG-RDG (c, g) hydrogels 28 days post-implantation in subcutaneous pockets of C57BL/6 mice. The images show H&E (a–c), and Masson's Trichrome (e–g) and stained dorsal tissue sections. The # denotes the location of the implant, which was lost during processing. Arrows mark the location of the fibrous capsule. The scale bar is 100μm. Thickness of the inflammatory cell layer (d), thickness of the fibrous capsule (h), and relative collagen density in the fibrous capsule, where intensity was normalized to the intensity of the fibrous capsule surrounding the PEG hydrogel at the location closest to the implant (i.e., 0–10 microns) (i) were measured on the dorsal side of the implanted hydrogels. Data are presented as mean with standard deviation as error bars for n=5 biological replicates per hydrogel condition.

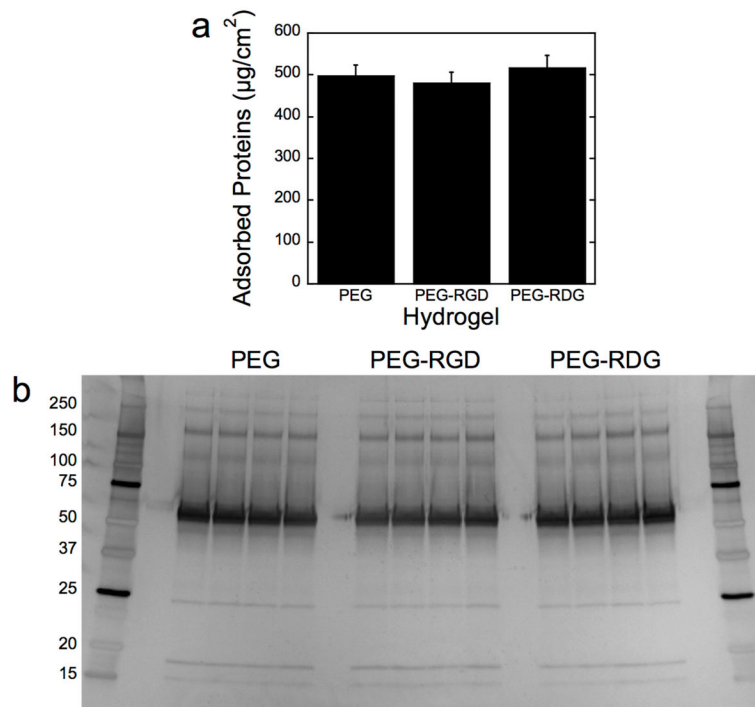


**Figure 2.** *In vitro* protein adsorption to PEG, PEG-RGD, and PEG-RDG hydrogels following a two-hour incubation in fetal bovine serum assessed by total protein mass (a) and protein signature (b). The latter is visualized via silver stained SDS-PAGE. Molecular weight ladders were run on both sides of the gel. Data are presented as mean with standard deviation as error bars (n=3).

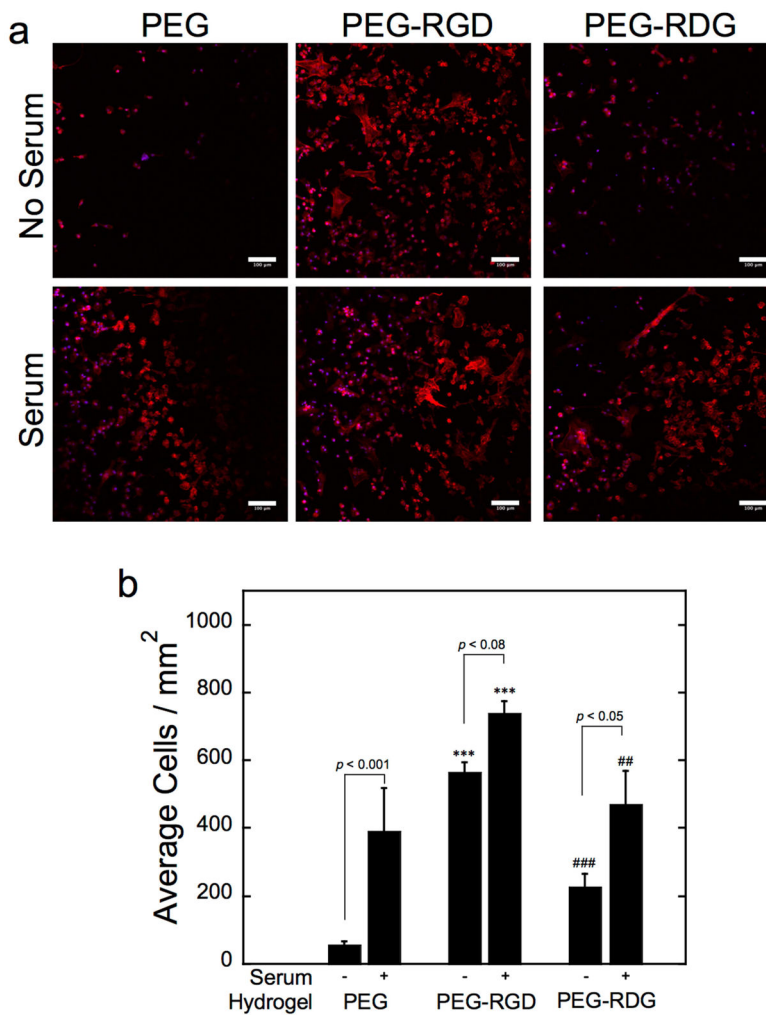


**Figure 3.** Representative confocal microscopy images (a) and semi-quantitative analysis (b) of macrophages attachment to PEG, PEG-RGD, and PEG-RDG hydrogels in the absence and presence of pre-adsorbed serum proteins. Scale bar is 100  $\mu$ m. Data are presented as mean with standard deviation as error bars (n=4). Symbols represent significance compared to PEG (\*) and PEG-RGD (#), where two symbols represent  $p < 0.01$  and three symbols represent  $p < 0.001$ .



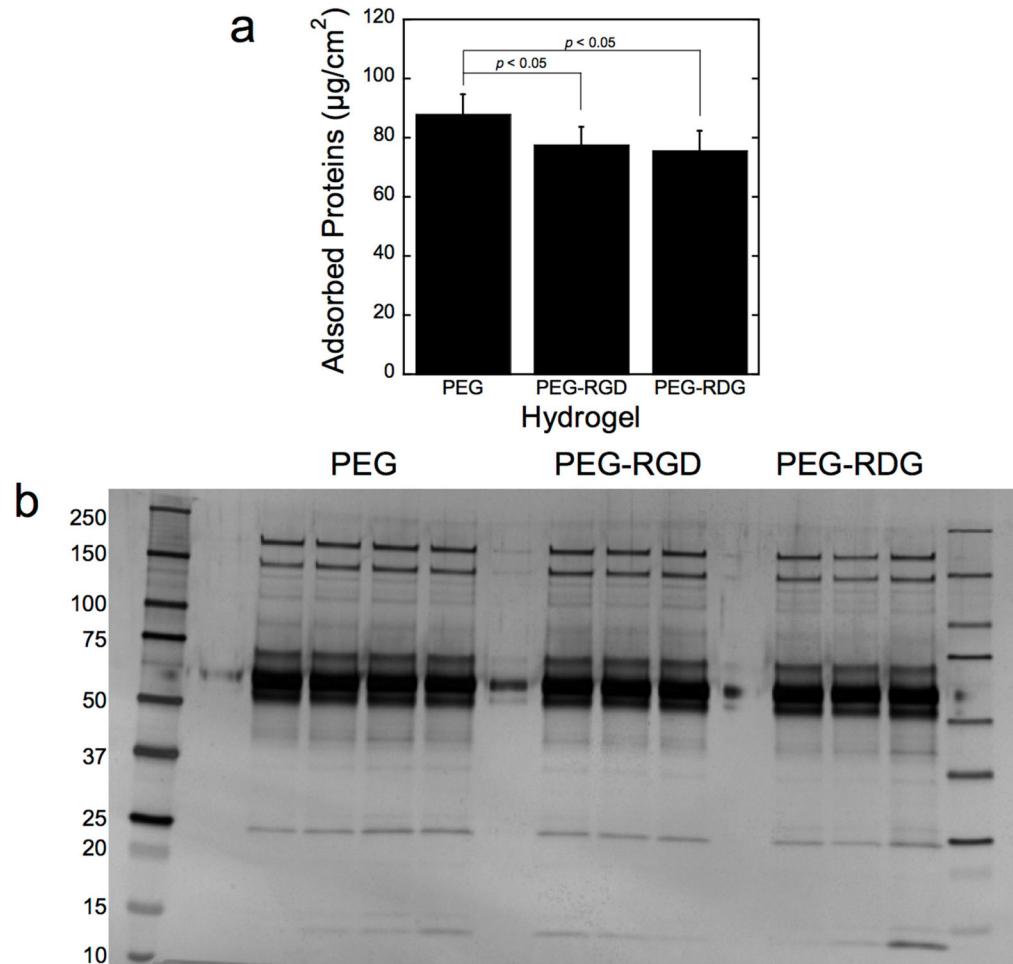


**Figure 4.**

*In vivo* protein adsorption to PEG, PEG-RGD, and PEG-RDG hydrogels following a 30 minute subcutaneous implantation into C57BL/6 mice by total protein mass (a) and protein signature (b). The latter is visualized via silver stained SDS-PAGE. Molecular weight ladders were run on both sides of the gel. Data are presented as mean with standard deviation as error bars for n=3–4 biological replicates per hydrogel condition.

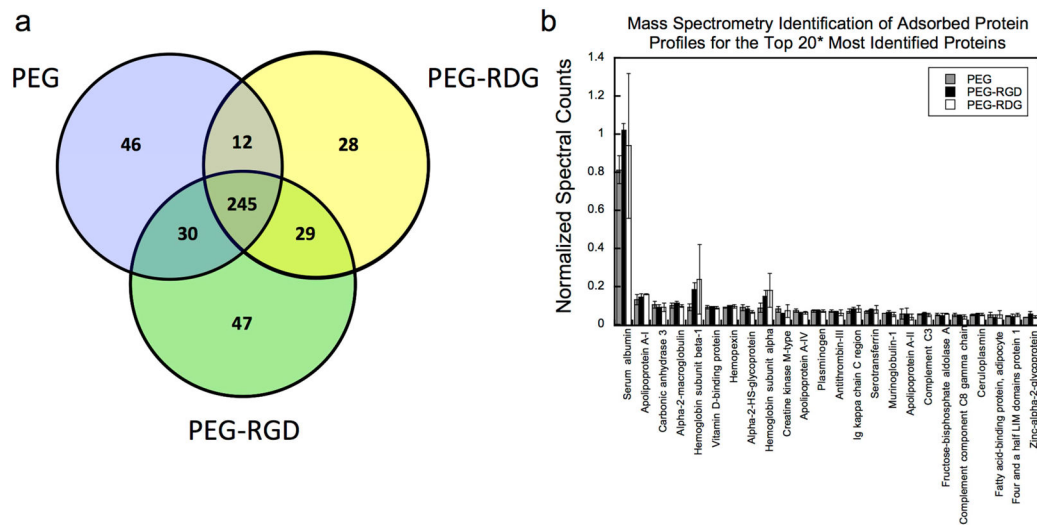


**Figure 5.**

A Venn diagram depicting the overlap of the top 90% of proteins that were identified adsorbed to PEG, PEG-RGD and PEG-RDG hydrogels (a). The top 20 most identified proteins for each PEG, PEG-RGD, and PEG-RDG hydrogel, which were quantified by normalizing spectral counts to protein length (i.e., number of amino acids) (b). The asterisks indicates the top 20 are presented for each hydrogel resulting in a total of 24 proteins that are presented. Data are presented as mean with standard deviation as error bars for n=3 biological replicates per hydrogel condition.

**Table 1**

Electron Spectroscopy for Chemical Analysis (ESCA)

Hydrogel	Elemental concentrations (%)		
	C 1s	O 1s	N 1s
PEG	69.2±1.0	30.8±1.1	0.07±0.12
PEG-RGD	68.0±0.4	31.5±0.5	0.48±0.12
PEG-RDG	67.3±1.2	31.2±1.3	0.49±0.16

Author Manuscript

Author Manuscript

Author Manuscript

Author Manuscript

Table 2

## GO Extracellular Space Terms

GO ID	Term	%*			
		PEG	PEG-RGD	PEG-RDG	PEG-RDG
GO:0005576	extracellular region	40.7	42.5	38.8	38.8
GO:0044421	extracellular region part	21.3	22.7	20.7	20.7
GO:0005615	extracellular space	18.8	20.1	18.6	18.6
GO:0005856	cytoskeleton	11.2	11.5	10.9	10.9
GO:0005829	cytosol	11.2	10.9	10.4	10.4
GO:0044430	cytoskeletal part	8.1	8.0	8.0	8.0
GO:0031410	cytoplasmic vesicle	6.5	6.2	6.4	6.4
GO:0031982	vesicle	6.5	6.2	6.4	6.4
GO:0016023	cytoplasmic membrane-bounded vesicle	6.2	5.9	6.1	6.1
GO:0031988	membrane-bounded vesicle	6.2	5.9	6.1	6.1
GO:0031012	extracellular matrix	5.1	5.3	4.8	4.8
GO:0042470	melanosome	4.8	4.7	5.0	5.0
GO:0048770	pigment granule	4.8	4.7	5.0	5.0

\* percent of the total proteins identified that are involved in each term.

Table 3

## GO Biological Process

<i>GO ID</i>	<i>Term</i>	<i>PEG</i>	<i>PEG-RGD</i>	<i>PEG-RDG</i>	<i>%*</i>
GO:0009611	response to wounding	16.6	17.1	15.2	
GO:0006508	proteolysis	15.7	15.0	14.1	
GO:0006952	defense response	14.0	14.7	12.8	
GO:0006955	immune response	11.2	12.1	10.9	
GO:0006954	inflammatory response	11.0	12.1	10.4	
GO:0002526	acute inflammatory response	10.4	11.5	9.8	
GO:0048584	positive regulation of response to stimulus	9.3	9.1	8.5	
GO:0002684	positive regulation of immune system process	9.0	9.1	7.7	
GO:0002252	immune effector process	8.4	8.8	7.7	
GO:0050778	positive regulation of immune response	8.4	8.8	7.7	
GO:0042592	homeostatic process	8.4	8.6	9.0	
GO:0006959	humoral immune response	7.9	8.3	7.4	
GO:0010033	response to organic substance	7.9	8.3	8.0	
GO:0055114	oxidation reduction	7.9	8.0	8.5	
GO:0002253	activation of immune response	7.6	8.0	6.9	
GO:0051604	protein maturation	7.6	7.7	7.2	
GO:0045087	innate immune response	7.6	7.4	6.9	
GO:0005996	monosaccharide metabolic process	7.3	7.4	7.2	
GO:0006956	complement activation	7.0	7.4	6.6	
GO:0002541	activation of plasma proteins involved in acute inflammatory response	7.0	7.4	6.6	
GO:0051605	protein maturation by peptide bond cleavage	7.0	7.4	6.6	
GO:0016485	protein processing	7.0	7.1	6.6	
GO:0019318	hexose metabolic process	7.0	7.1	6.9	
GO:0002449	lymphocyte mediated immunity	6.7	7.1	6.4	
GO:0002443	leukocyte mediated immunity	6.7	6.8	6.4	
GO:0006006	glucose metabolic process	6.7	6.8	6.6	
GO:0006091	generation of precursor metabolites and energy	6.7	6.8	6.4	

<i>GO ID</i>	<i>Term</i>	PEG	PEG-RGD	PEG-RDG
GO:0002455	humoral immune response mediated by circulating immunoglobulin	6.5	6.8	6.1
GO:0016064	immunoglobulin mediated immune response	6.5	6.8	6.1
GO:0019724	B cell mediated immunity	6.5	6.8	6.1
GO:0002250	adaptive immune response	6.5	6.8	6.1
GO:0002460	adaptive immune response based on somatic recombination of immune receptors built from immunoglobulin superfamily domains	6.5	6.5	6.1
GO:0042060	wound healing	6.5	6.5	5.6
GO:0019725	cellular homeostasis	6.2	6.5	6.1
GO:0006958	complement activation, classical pathway	5.9	6.2	5.6
GO:0016052	carbohydrate catabolic process	5.9	6.2	6.1
GO:0042981	regulation of apoptosis	5.9	6.2	6.4
GO:0043067	regulation of programmed cell death	5.9	6.2	6.4
GO:0010941	regulation of cell death	5.9	5.9	6.6
GO:0044275	cellular carbohydrate catabolic process	5.3	5.6	5.3
GO:0050817	coagulation	5.3	5.6	4.8
GO:0007596	blood coagulation	5.3	5.6	4.8
GO:0007599	hemostasis	5.3	5.6	4.8
GO:0050878	regulation of body fluid levels	5.3	5.6	4.8
GO:0046164	alcohol catabolic process	5.1	5.3	5.1
GO:0006007	glucose catabolic process	4.8	5.0	4.8
GO:0019320	hexose catabolic process	4.8	5.0	4.8
GO:0046365	monosaccharide catabolic process	4.8	5.0	4.8

\* percent of the total proteins identified that are involved in each term.